A critical role for PPARα-mediated lipotoxicity in the pathogenesis of diabetic cardiomyopathy: Modulation by dietary fat content

Brian N. Finck*, Xianlin Han*, Michael Courtois*, Franck Aimond†, Jeanne M. Nerbonne†, Attila Kovacs*, Richard W. Gross*†, and Daniel P. Kelly*†‡§

Departments of *Medicine, †Molecular Biology and Pharmacology, and ‡Pediatrics, Center for Cardiovascular Research, Washington University School of Medicine, St. Louis, MO 63110

Edited by Roger H. Unger, University of Texas Southwestern Medical Center, Dallas, TX, and approved December 5, 2002 (received for review November 1, 2002)

To explore the role of peroxisome proliferator-activated receptor α (PPARα)-mediated derangements in myocardial metabolism in the pathogenesis of diabetic cardiomyopathy, insulinopenic mice with PPARα deficiency (PPAR$\alpha^{-/-}$) or cardiac-restricted overexpression [myosin heavy chain (MHC)-PPAR] were characterized. Whereas PPAR$\alpha^{-/-}$ mice were protected from the development of diabetes-induced cardiac hypertrophy, the combination of diabetes and the MHC-PPAR genotype resulted in a more severe cardiomyopathic phenotype than either did alone. Cardiomyopathy in diabetic MHC-PPAR mice was accompanied by myocardial long-chain triglyceride accumulation. The cardiomyopathic phenotype was exacerbated in MHC-PPAR mice fed a diet enriched in triglyceride containing long-chain fatty acid, an effect that was reversed by discontinuing the high-fat diet and absent in mice given a medium-chain triglyceride-enriched diet. Reactive oxygen intermediates were identified as candidate mediators of cardiomyopathic effects in MHC-PPAR mice. These results link dysregulation of the PPARα gene regulatory pathway to cardiac dysfunction in the diabetic and provide a rationale for serum lipid-lowering strategies in the treatment of diabetic cardiomyopathy.

Results of epidemiologic studies indicate that diabetic individuals are at an extraordinarily high risk for the development of cardiovascular disease. The prevalence of risk factors including hyperlipidemia and hypertension certainly contribute to the high incidence of cardiovascular disease in the diabetic population. However, myocardial dysfunction (diabetic cardiomyopathy) is common in diabetic individuals independent of hypertension and coronary artery disease (1). In addition, morbidity and mortality after myocardial infarction is significantly greater in diabetic compared with nondiabetic patients (2). Although the pathogenesis of diabetic cardiomyopathy is poorly understood, recent evidence implicates perturbations in cardiac energy metabolism. Whereas mitochondrial fatty acid oxidation (FAO) is the chief energy source for the normal postnatal mammalian heart, the relative contribution of glucose utilization pathways is significant, allowing the plasticity necessary for steady ATP production in the context of diverse physiologic and dietary conditions (3). Because of the importance of insulin in the regulation of myocardial metabolism, chronic insulin deficiency or resistance results in a marked reduction in cardiac glucose utilization such that the heart relies almost exclusively on fatty acids to generate energy (4, 5). High rates of fatty acid utilization in the diabetic heart could lead to functional derangements related to accumulation of lipid intermediates, mitochondrial or peroxisomal generation of reactive oxygen species, or excessive oxygen consumption.

Recently, we found that the diabetes-induced shift in cardiac fuel preference is associated with activation of the peroxisome proliferator-activated receptor (PPAR) α gene regulatory system (6). PPARα is a nuclear receptor that regulates the transcription of an array of genes involved in cellular fatty acid utilization pathways including transport, esterification, and oxidation (reviewed in refs. 7 and 8). The cardiac expression and activity of PPARα and its coactivator PGC-1α are increased in rodent models of insulin-deficient and insulin-resistant diabetes (6). Transgenic mice with cardiac-specific overexpression of PPARα [myosin heavy chain (MHC)-PPAR mice] were recently shown to recapitulate many of the metabolic abnormalities of the diabetic heart, including increased fatty acid utilization and reduced glucose uptake (6). The development of cardiomyopathy in MHC-PPAR mice indicated that whereas increased fat utilization in the diabetic heart may initially serve a compensatory role to maintain ATP production, chronic derangements in myocardial metabolism may have maladaptive consequences, including functional abnormalities. Accordingly, the MHC-PPAR mouse provided us the opportunity to evaluate the role of PPARα-mediated derangements in cardiac lipid metabolism in the development of diabetic cardiomyopathy.

Methods

Animal Studies. All studies were approved by the Animal Studies Committee of Washington University School of Medicine. Transgenic MHC-PPAR mice have been described (6). Two independent lines of MHC-PPAR mice (*404-4, 404-3*) were used. Functional and metabolic endpoints were analyzed in littermate transgenic and nontransgenic (NTG) mice. PPARα-null (PPAR$\alpha^{-/-}$) and wild-type control (PPAR$\alpha^{+/+}$) mice have been described (9).

Mice were rendered insulin-deficient by a single i.p. injection of streptozotocin [STZ; Sigma; 180 mg/kg body weight (BW)], as described (6). Diabetes (blood glucose >250 mg/dl) was confirmed by tail blood glucose monitoring (B-GLUCOSE Analyzer; Hemocue, Angelholm, Sweden).

MHC-PPAR and NTG littermate animals were administered high-fat (HF) diet providing 43% of the calories from fat (TD 97268, Harlan Teklad, Madison, WI) or an isocaloric control chow providing 14% calories from fat (TD 97267, Harlan Teklad). To determine the impact of fatty acid chain length, mice were administered HF chow (43% of calories from fat) containing triacylglyceride (TAG) comprised of medium-chain (MCT) fatty acids (8:0 and 10:0; TD 00308) or matched long-chain (LCT) fatty acids (16:0 and 18:1; TD 01381). The length of studies varied as described in *Results*.

This paper was submitted directly (Track II) to the PNAS office.

Abbreviations: FAO, fatty acid oxidation; ESIMS, electrospray ionization MS; PPAR, peroxisome proliferator-activated receptor; NTG, nontransgenic; STZ, streptozotocin; HF, high-fat; MHC, myosin heavy chain; TAG, triacylglyceride; MCT, medium-chain TAG; LCT, long-chain TAG; LCFA, long-chain fatty acid; ACO, acyl-CoA oxidase; GSH, glutathione; GSSG, oxidized GSH; BW, body weight; BV, biventricular; LV, left ventricular.

§To whom correspondence should be addressed at: Center for Cardiovascular Research, Washington University School of Medicine, 660 South Euclid Avenue, Campus Box 8086, St. Louis, MO 63110. E-mail: dkelly@im.wustl.edu.

 www.pnas.org/cgi/doi/10.1073/pnas.0336724100

To inhibit mitochondrial import of long-chain fatty acid (LCFA), mice were injected i.p. with the + enantiomer of etomoxir (25 ng/kg) or vehicle (sterile water) daily for 3 weeks. During this 3-week period, mice were fed either HF or control chow.

Isolation of Cardiac Myocytes and Electrophysiologic Studies. Adult cardiac ventricular myocytes were isolated, and whole-cell voltage-clamp recordings were obtained by using an Axopatch 1D patch-clamp amplifier and the PCLAMP 8 software package (Axon Instruments, Foster City, CA), as described (10). Further description of these and other methods is found in *Supporting Text*, which is published as supporting information on the PNAS web site, www.pnas.org.

Echocardiographic Studies. Transthoracic M-mode and two-dimensional echocardiography were performed on conscious mice by using an Acuson Sequoia 256 Echocardiography system (Acuson, Mountain View, CA), as described (11). Methods for measurements of LV mass and chamber size using M-mode have been described (11).

Histologic Analyses. After harvest, a mid-ventricular slice of myocardium was snap-frozen in a cryomold for sectioning or preserved in buffered formalin. To detect neutral lipid, frozen sections were stained with oil red O and counterstained with hematoxylin. To detect signs of fibrosis, sections were stained with Gomori's trichrome.

Analysis of Myocardial TAG and Ceramide Levels. The quantitative analysis of myocardial TAG species (12) and ceramide (13) by electrospray ionization mass spectrometry (ESIMS) has been described.

Northern Blotting Analyses. Northern blotting analyses were performed as described (14) by using radiolabeled cDNA probes for murine acyl-CoA oxidase (ACO) and human glyceraldehyde-3-phosphate dehydrogenase.

Analyses of H_2O_2 Levels and Reduced/Oxidized Glutathione (GSH) Ratios. Hydrogen peroxide levels (15) and reduced GSH and oxidized GSH (GSSG) levels (16) were determined as described.

Statistical Analysis. Statistical comparisons were made by using unpaired *t* test or ANOVA coupled to Scheffé's test when appropriate. All data are presented as means ± SEM, with a statistically significant difference defined as a value of $P < 0.05$.

Results

The Expression of the Diabetic Cardiomyopathic Phenotype Is Influenced by the Activity of PPARα. To determine whether the PPARα regulatory pathway is necessary for the cardiomyopathic effects of diabetes, the ventricular hypertrophic response was evaluated in PPARα-null ($PPAR\alpha^{-/-}$) and strain-matched wild-type ($PPAR\alpha^{+/+}$) mice rendered insulin-deficient by administration of STZ. Insulin deficiency caused a marked reduction in BW 6 weeks after STZ injection (Table 1, which is published as supporting information on the PNAS web site). However, the biventricular (BV) weight to BW ratio was significantly increased in diabetic $PPAR\alpha^{+/+}$ mice but not in diabetic $PPAR\alpha^{-/-}$ mice (Fig. 1*a*). Echocardiographic analyses also demonstrated an increase in LV mass index in $PPAR\alpha^{+/+}$ mice but not in $PPAR\alpha^{-/-}$ mice after STZ treatment (Table 1). There was no significant difference in left ventricular (LV) function or cavity dimension in STZ-treated $PPAR\alpha^{+/+}$ or $PPAR\alpha^{-/-}$ mice compared with vehicle-treated controls (data not shown). To evaluate the hypertrophic response independent of changes in BW, whole-cell membrane capacitance (C_m) was used as a measure of myocyte volume in cardiomyocytes isolated from diabetic mice. Consistent with the increased BV/BW ratio in diabetic $PPAR\alpha^{+/+}$ but not in $PPAR\alpha^{-/-}$ mice, the C_m of myocytes isolated from diabetic $PPAR\alpha^{+/+}$ mice was significantly increased compared with saline-treated controls, whereas no difference in C_m was detected between diabetic and nondiabetic $PPAR\alpha^{-/-}$ myocytes (Fig. 1*a*). The input resistances of isolated cardiomyocytes was not affected by genotype or by diabetes, indicating that cell viability was normal (0.93–1.1 GΩ).

Next, we sought to determine whether insulin deficiency would influence the severity of cardiomyopathy exhibited by mice with cardiac-restricted overexpression of PPARα (MHC-PPAR mice). As expected, the BV/BW ratio was increased in diabetic mice compared with vehicle-treated controls 6 weeks after STZ administration (Fig. 1*b*). However, the increase in BV/BW ratio exhibited by diabetic MHC-PPAR mice was markedly greater than that observed in NTG mice (Fig. 1*b*). More importantly, echocardiographic analysis demonstrated that in contrast to

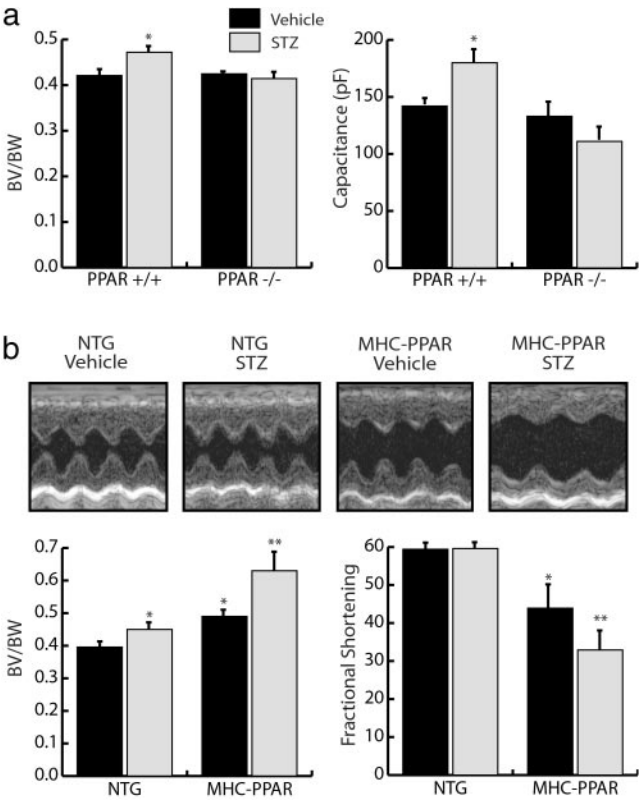

Fig. 1. The diabetic cardiac phenotype is influenced by the activity of PPARα. (*a*) PPARα-null mice are resistant to development of diabetic ventricular hypertrophy. (*Left*) Bars represent mean (± SEM) BV/BW ratios ($n \geq 11$) of $PPAR\alpha^{+/+}$ and $PPAR\alpha^{-/-}$ mice 6 weeks after an injection of vehicle or STZ. (*Right*) Bars represent mean cellular capacitance ($n \geq 12$) of isolated cardiomyocytes from $PPAR\alpha^{+/+}$ and $PPAR\alpha^{-/-}$ mice 6 weeks after injection of vehicle or STZ. *, $P < 0.05$ vs. vehicle-injected $PPAR\alpha^{+/+}$ and all $PPAR\alpha^{-/-}$ mice. (*b*) Ventricular hypertrophy and dysfunction are exacerbated in diabetic MHC-PPAR mice (*Lower Left*). Bars represent mean (± SEM) BV/BW ratios ($n \geq 7$) of MHC-PPAR and NTG littermate mice after an injection of saline vehicle or STZ. (*Lower Right*) Bars represent mean percent LV fractional shortening ($n \geq 7$ for each group) as assessed by echocardiographic analysis 6 weeks after an injection of vehicle or STZ. *, $P < 0.05$ vs. vehicle-injected NTG mice. **, $P < 0.05$ vs. NTG mice and vehicle-injected MHC-PPAR mice. (*Upper*) Representative two-dimensional guided M-mode images of the LV obtained from the parasternal view at the mid-ventricular level of control and diabetic NTG and MHC-PPAR mice.

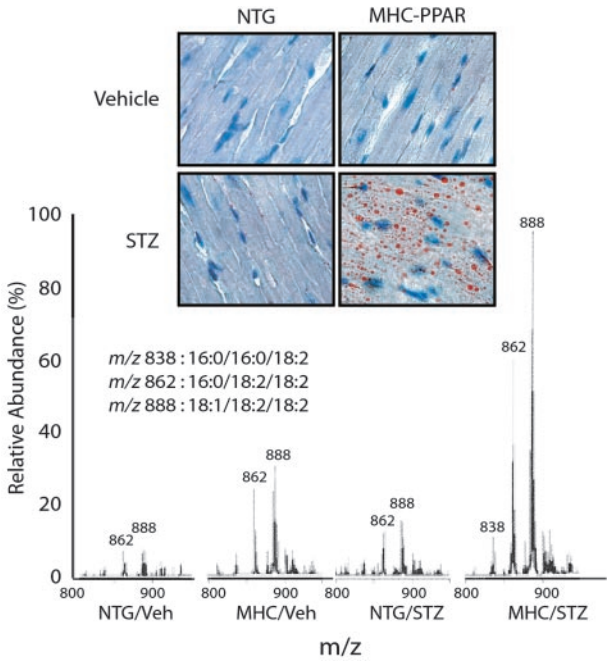

Fig. 2. Myocardial TAG accumulation in diabetic MHC-PPAR mice. (*Upper*) Photomicrographs depicting the histologic appearance of ventricular tissue from NTG and MHC-PPAR mice (*404-3* line) after an injection of vehicle or STZ are shown. Red droplets indicate neutral lipid staining. (*Lower*) Representative spectra from ESIMS analyses for linoleic acid-containing TAGs. *m/z* ratios of 838, 862, and 888 denote TAGs containing acyl groups with chain lengths of 16:0/16:0/18:2, 16:0/18:2/18:2, and 18:1/18:2/18:2, respectively.

NTG mice, LV fractional shortening (FS) was significantly reduced in diabetic MHC-PPAR mice (Fig. 1*b*). Collectively, the results of the PPARα gain-of-function and loss-of-function studies indicate that activation of the PPARα regulatory pathway is critical to the cardiomyopathic response of the diabetic heart.

Myocardial TAG Levels Parallel Cardiac Dysfunction Caused by Diabetes and PPARα Overexpression. Accumulation of lipid within cardiac myocytes is a histologic hallmark of the diabetic heart (17–19). Elevated circulating levels of free fatty acids and TAG-rich lipoproteins in combination with increased capacity for myocardial fatty acid uptake likely act in concert to cause myocyte lipid accumulation in diabetics. Neutral lipid accumulation as determined by oil red O staining was markedly greater within the myocytes of diabetic MHC-PPAR mice compared with that of all other treatment groups (Fig. 2). Quantification of myocardial TAG species by ESIMS demonstrated that levels of TAG containing LCFA were significantly elevated in vehicle-treated MHC-PPAR and diabetic NTG mice compared with vehicle-treated NTG mice, and that this effect was strikingly amplified in diabetic MHC-PPAR mice (Fig. 2). Examination of the profile of TAG species in the diabetic MHC-PPAR heart revealed marked increases in TAG-containing LCFA species, including palmitic, oleic, and linoleic acids, a profile similar to that of insulin-deficient NTG mice (Fig. 6, which is published as supporting information on the PNAS web site) and to that found in the standard chow diet and plasma (data not shown). These results demonstrate that myocardial LCFA levels correlate with the cardiomyopathic phenotype in diabetic MHC-PPAR mice.

HF Diet Potentiates Cardiac Dysfunction in MHC-PPAR Mice in a Reversible Manner. To determine whether increased delivery of lipid to the myocardium, such as occurs in the uncontrolled diabetic state, contributes to the development of cardiomyopathy, nondiabetic NTG and MHC-PPAR mice were fed a chow that provided 43% of its calories as LCFA (HF diet) or an isocaloric control chow containing 14% calories as fat for 4 weeks. The initial experiments were performed with the MHC-PPAR line exhibiting the lowest level of transgene expression (line *404-4*; ref. 6), because ventricular hypertrophy and dysfunction are minimal in this transgenic line. No difference in BW was detected between HF and control chow-fed mice (Table 2, which is published as supporting information on the PNAS web site). Although the HF diet had no effect on ventricular weight or function in NTG animals, a robust increase in ventricular weight, ventricular chamber dilatation, and a significant decline in the fractional shortening was detected in HF-fed MHC-PPAR mice (Fig. 3*a* and Table 2). Cardiac functional indices were similarly affected by HF diet when mice with higher transgene expression (*404-3* line) were used in identical experiments (Table 2). Coincident with cardiac dysfunction and hypertrophy, ESIMS analyses revealed striking accumulation of TAG comprised of palmitic, oleic, and linoleic acids in MHC-PPAR, but not NTG mice fed HF chow (Fig. 3*b*). Ceramide and related downstream pathways have been identified as mediators of cardiac myocyte injury and death in other cardiomyopathic states. HF diet administration significantly increased myocardial ceramide levels in transgenic mice but not wild-type mice, thus providing further evidence that LCFA metabolic pathways are stimulated in the MHC-PPAR heart (Fig. 3*b*).

To evaluate the reversibility of the HF diet-induced cardiomyopathy in MHC-PPAR mice, HF chow was administered for 4 or 8 weeks. Then, in subgroups of mice, the HF diet was replaced with control chow for an additional 2 weeks. Remarkably, in both the 4- and 8-week groups, the ventricular dysfunction of MHC-PPAR mice on the HF chow was reversed to the level of control chow-fed MHC-PPAR mice 2 weeks after returning to the standard rodent chow (Fig. 3*c*). Mean LV internal diameter at diastole (LVIDd), a measure of LV chamber dimension, was increased vs. baseline in MHC-PPAR mice fed HF chow for 8 weeks. This increase was significantly improved by return to standard chow ($P < 0.05$) (baseline, 3.37 $\pm$ 0.20 mm; 8 weeks HF, 4.00 $\pm$ 0.08 mm; 2 weeks post-HF, 3.80 $\pm$ 0.03 mm). The HF diet-induced LV hypertrophy was not reversed by removal of the HF diet during the same time period (data not shown). ESIMS analyses revealed that discontinuation of the HF feeding also resulted in a reduction of myocardial TAG levels to that of control-fed transgenic mice (data not shown). Despite the fact that MHC-PPAR myocardial ceramide levels were increased (Fig. 3*b*) and cardiac function decreased on the HF diet, histological staining for markers of apoptotic death (terminal deoxynucleotidyltransferase-mediated dUTP and activated caspase-3) revealed no evidence of abnormal myocyte apoptosis (data not shown). Furthermore, after 8 weeks on the HF diet, trichrome staining of MHC-PPAR cardiac sections demonstrated myocyte hypertrophy but no significant fibrosis, which is consistent with the absence of significant myocyte death (Fig. 7, which is published as supporting information on the PNAS web site). Taken together, these results suggest that the "lipotoxic" effect was reversible, at least in the short term.

Medium-Chain HF Diet Rescues Cardiac Dysfunction in MHC-PPAR Mice. The observed influence of long-chain HF diet on the cardiomyopathic phenotype of MHC-PPAR mice could be related to the toxic effects of LCFA moieties or it could be secondary to increased oxidation rates *per se*. As an initial step in distinguishing between these possibilities, MHC-PPAR mice were fed an isocaloric standard chow or matched HF diets enriched in MCT (octanoate and decanoate) or LCT for 8 weeks. The rationale for MCT chow administration was to maintain high rates of mitochondrial FAO in the absence of

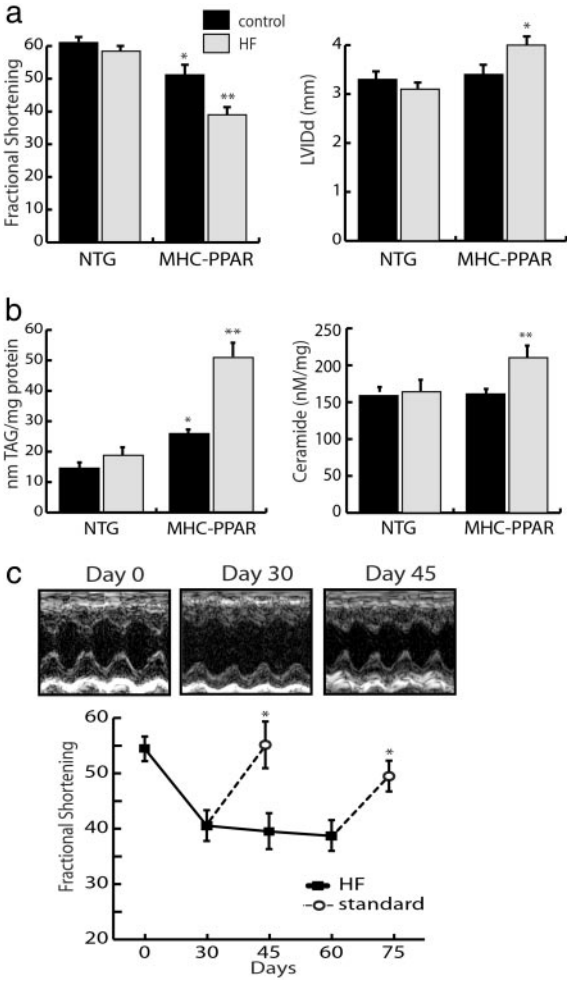

Fig. 3. The cardiomyopathy of MHC-PPAR mice is worsened by consumption of a diet rich in LCFA. (*a*) Bars represent mean LV FS (*Left*) and LV internal diameter at diastole (LVIDd, *Right*) of NTG and MHC-PPAR (*404-4* line) mice on HF chow rich in LCFA or calorie-matched control chow. (*b*) TAG and ceramide levels in hearts of NTG and MHC-PPAR mice after HF diet treatment, as determined by ESIMS. Bars represent mean levels of long-chain TAG (*Left*) and ceramide (*Right*). *, $P < 0.05$ vs. NTG mice. **, $P < 0.05$ vs. NTG mice and control chow-fed MHC-PPAR mice. (*c*) HF diet-induced ventricular dysfunction in MHC-PPAR mice is reversible. The graph displays mean FS of MHC-PPAR mice plotted as a function of time. Black squares represent transgenic mice fed the HF diet. Subgroups of mice returned to a standard rodent chow for 15 days at the 30th and 60th days of the trial are denoted by the white circles. *, $P < 0.05$ vs. corresponding HF-fed MHC-PPAR mice. (*Upper*) M-mode echocardiographic images of the LV of a representative MHC-PPAR mouse at baseline (Day 0), after 30 days on the HF diet (Day 30) and 15 days after being returned to the standard chow (Day 45).

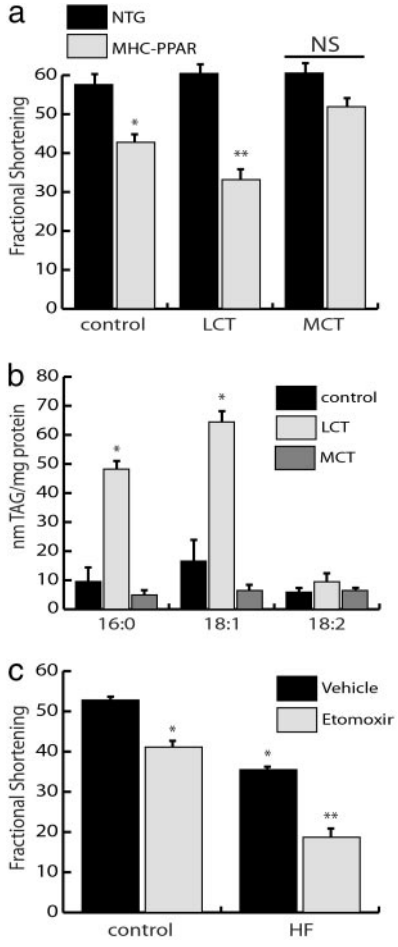

Fig. 4. Diet-induced cardiac lipotoxicity depends upon fatty acid chain length but does not require increased flux of fatty acids through mitochondrial pathways. (*a*) MCT diet rescues cardiac dysfunction in MHC-PPAR mice. Bars represent mean echocardiographic-determined LV fractional shortening of NTG and MHC-PPAR mice (*404-3* line; $n \geq 5$ for each group) 8 weeks after initiation of control, LCT, or MCT diet administration. *, $P < 0.05$ vs. NTG mice. **, $P < 0.05$ vs. NTG mice and MHC-PPAR mice on control or MCT chows. NS = nonsignificant. (*b*) LCT but not MCT HF diet increases myocardial TAG levels. Bars represent mean levels of TAG-associated fatty acids with chain length of 16:0, 18:1, and 18:2 in MHC-PPAR mouse ventricles after 8 weeks of control, LCT, or MCT diet administration. *, $P < 0.05$ vs. MHC-PPAR mice fed control or MCT chow. (*c*) Inhibition of mitochondrial fatty acid import exacerbates cardiac dysfunction in MHC-PPAR mice. Fractional shortening of MHC-PPAR mice (*404-4* line; $n \geq 5$ for each group) after 3 weeks of daily injections of etomoxir sodium (25 ng/kg/day) while receiving control or HF chow. *, $P < 0.05$ vs. MHC-PPAR mice on control chow. **, $P < 0.05$ vs. MHC-PPAR mice on control chow and saline-treated HF mice.

LCFA intermediate accumulation. As expected, LCT administration exacerbated cardiac hypertrophy, ventricular chamber dilatation, and contractile dysfunction in MHC-PPAR mice (Fig. 4*a*). In contrast, cardiomyopathy did not develop in MCT diet-fed MHC-PPAR mice. In fact, the MCT diet rescued the baseline ventricular function of MHC-PPAR mice to normal levels (Fig. 4*a*). ESIMS analyses of cardiac lipid extracts revealed that LCT diet increased levels of TAG containing palmitate and oleate but not linoleic acid (Fig. 4*b*). This is reflective of dietary fat content, because the LCT diet contains only low levels of linoleic acid. Conversely, the MCT diet did not lead to accumulation of MCT or LCT (Fig. 4*b*).

Activation of Extra-Mitochondrial Lipid Metabolic Pathways in MHC-PPAR Heart. The results of the MCT diet studies suggested that lipid metabolic pathways upstream of the mitochondrial FAO cycle were involved in the development of cardiomyopathy. To investigate the effects of inhibiting mitochondrial import of LCFA, MHC-PPAR mice were treated for 3 weeks with etomoxir, a pharmacological inhibitor of carnitine palmitoyltransferase I, which catalyzes a necessary step in mitochondrial import of LCFA. Although, etomoxir treatment did not adversely affect ventricular function in NTG mice (data not shown), inhibition of long-chain FAO caused a significant deterioration in cardiac function in MHC-PPAR mice given control chow (Fig. 4*c*). In the context of the HF chow, etomoxir treatment led to striking LV dysfunction and clinical evidence of heart failure, including

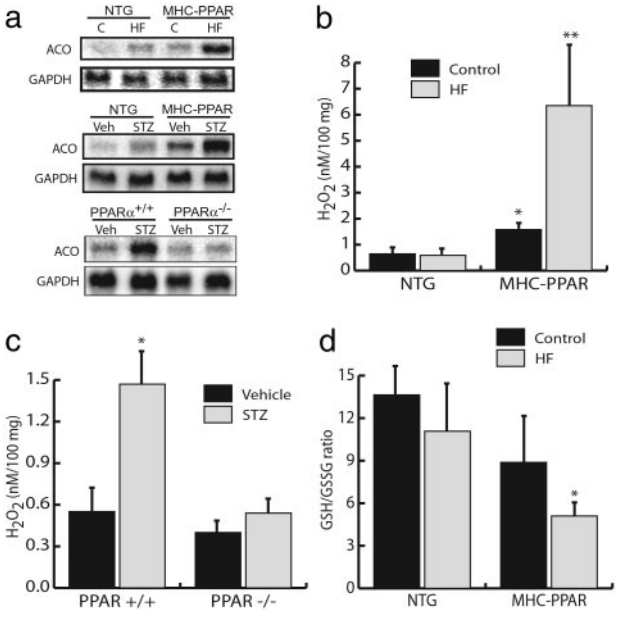

Fig. 5. Activation of extra-mitochondrial lipid metabolic pathways correlates with the severity of the cardiomyopathic phenotype. (*a*) HF diet or STZ treatment activates the peroxisomal FAO pathway in a PPARα-dependent manner. Representative autoradiographs of Northern blot analyses performed with total RNA isolated from cardiac ventricle of NTG or MHC-PPAR mice after 4 weeks of HF or control (C) diet (*Top*), NTG or MHC-PPAR mice 6 weeks after STZ administration (*Middle*), PPAR$\alpha^{+/+}$ and PPAR$\alpha^{-/-}$ mice 5 days after vehicle or STZ injection (*Bottom*) using cDNA probes denoted at left. (*b*) Bars represent mean hydrogen peroxide (H_2O_2) levels in cardiac extracts from NTG or MHC-PPAR mice after 4 weeks of HF diet. *, $P < 0.05$ vs. NTG mice. **, $P < 0.05$ vs. NTG mice and MHC-PPAR mice fed control chow. (*c*) PPARα is required for the generation of H_2O_2 in the diabetic heart. Bars represent mean H_2O_2 levels in cardiac extracts isolated from PPAR$\alpha^{+/+}$ and PPAR$\alpha^{-/-}$ mice 5 days after an injection of vehicle or STZ. *, $P < 0.05$ vs. vehicle-injected wild-type and all PPARα-null mice. (*d*) Bars represent mean GSH/GSSG ratios ($n \geq 4$) in cardiac extracts from MHC-PPAR mice after 4 weeks of control or HF diet. *, $P < 0.05$ vs. NTG mice given HF chow.

ventricular wall thinning, chamber dilatation, and severely reduced fractional shortening in MHC-PPAR mice (Fig. 4*c* and data not shown). These data strongly suggest that extra-mitochondrial accumulation or metabolism of LCFA moieties lead to cardiac dysfunction in the MHC-PPAR model of diabetic cardiomyopathy.

Studies were then performed to determine whether peroxisomal lipid metabolic pathways were activated in hearts of MHC-PPAR mice. In contrast to the mitochondrial FAO pathway, which generates reducing equivalents for oxidative phosphorylation, peroxisomal FAO couples electrons to the formation of hydrogen peroxide (H_2O_2). The peroxisomal FAO pathway is a known target of the PPARα regulatory system. The expression of the gene encoding ACO, which catalyzes the initial, rate-limiting step in peroxisomal β-oxidation, was therefore evaluated. ACO mRNA levels were increased in MHC-PPAR mice at baseline and induced in long-chain HF-fed or diabetic NTG mice, compared with NTG controls (Fig. 5*a*). Furthermore, administration of HF diet or insulinopenia led to a superinduction in ACO gene expression in transgenic mice (Fig. 5*a*). H_2O_2 is a potential myocyte toxin either directly or indirectly. To evaluate cardiac H_2O_2 levels, an assay based on horseradish peroxidase-mediated, H_2O_2-dependent oxidation of phenol red (15) was performed with ventricular lysates. Levels of H_2O_2 paralleled ACO gene expression and the development of cardiomyopathy, with highest levels observed in the hearts of MHC-PPAR mice given an HF diet (Fig. 5*b*).

To evaluate further the possibility that PPARα-mediated activation of the peroxisomal pathway is linked to the development of cardiomyopathy, ACO gene expression and H_2O_2 levels were evaluated in diabetic wild-type and PPAR$\alpha^{-/-}$ mice. Diabetes caused a significant increase in cardiac ACO mRNA and H_2O_2 levels in PPAR$\alpha^{+/+}$ mice (Fig. 5 *a* and *c*). In striking contrast, PPAR$\alpha^{-/-}$ mice rendered insulin-deficient did not exhibit increased cardiac ACO expression or H_2O_2 levels compared with controls (Fig. 5 *a* and *c*). These latter results correlated with the lack of a chronic hypertrophic response induced by STZ (see Fig. 1*a*).

The observation of increased H_2O_2 levels in the hearts of HF-fed MHC-PPAR mice suggested that the net level of cellular oxidative species was elevated. To examine MHC-PPAR hearts for evidence of oxidative stress, the ratio of reduced (GSH) to oxidized (GSSG) glutathione was determined. Although a trend toward reduced GSH/GSSG ratio was observed in MHC-PPAR compared with NTG hearts on control chow, no significant difference was detected (Fig. 5*d*). However, in the context of the HF chow, the ratio of GSH/GSSG was significantly reduced in MHC-PPAR mice vs. NTG controls (Fig. 5*d*). Taken together, these findings strongly suggest that in addition to H_2O_2, other potentially toxic reactive species are generated by PPARα-mediated increases in extra-mitochondrial fatty acid catabolism.

Discussion

The incidence of cardiovascular events related to diabetes has increased to epidemic levels in the Western world. Despite the magnitude of this problem, little is known about the pathogenesis of myocardial dysfunction in the diabetic patient. In the current study, we have used loss-of-function and gain-of-function approaches to show that myocardial lipid metabolic derangements downstream of the PPARα gene regulatory pathway play a critical role in the development of ventricular hypertrophy and dysfunction in the diabetic heart. The development of severe cardiomyopathy in diabetic MHC-PPAR mice was associated with marked myocardial lipid accumulation. Remarkably, administration of a diet enriched in LCFA exacerbated cardiomyopathy and lipid accumulation in MHC-PPAR mice in a reversible manner, whereas a medium-chain-rich HF diet rescued these abnormalities. Finally, we provide evidence that the cardiotoxic effects of HF diet feeding are likely mediated by intracellular toxins generated independently of mitochondrial FAO pathways, peroxisomal-generated H_2O_2 or other reactive oxygen species being candidate mediators.

Evidence is emerging that derangements in myocardial lipid metabolism lead to cardiac dysfunction in the insulin-resistant and diabetic heart. Histological analyses of diabetic hearts have revealed lipid droplet accumulation within cardiac myocytes (17–19). Transgenic mice with increased cardiac uptake of fatty acids due to overexpression of long-chain acyl-CoA synthetase develop cardiomyopathy (20). Studies performed with isolated working hearts of diabetic animals have demonstrated that high rates of FAO are associated with ventricular dysfunction (4, 5, 21). Recently, we have shown that chronic activation of the PPARα pathway (MHC-PPAR mice) leads to a marked increase in myocardial fatty acid uptake and oxidation, reduced glucose utilization, and cardiomyopathy, a metabolic and functional phenotype similar to that of the diabetic heart (6). Herein, we provide several lines of evidence to support the conclusion that lipid metabolic derangements mediated by the PPARα gene regulatory pathway lead to cardiac dysfunction in the diabetic heart. First, cardiac hypertrophy induced by insulin deficiency is prevented in PPARα-null mice. Conversely, the effects of insulin deficiency and PPARα overexpression are cooperative in the development of cardiomyopathy. Second, the cardiomyopathy in diabetic and MHC-PPAR mice is associated with the accumulation of TAG-containing LCFA. The profile of myocardial

TAG species was similar to the species of lipid in circulation, strongly suggesting that the expanded reservoir of TAG species represents increased fatty acid uptake. Third, the cardiomyopathy in MHC-PPAR mice worsened with administration of a diet enriched in TAG containing LCFA and was rescued by substitution of dietary LCFA with medium-chain fatty acids. Taken together, these results implicate direct or indirect toxic effects of LCFA in the development of diabetic cardiomyopathy, as modeled by MHC-PPAR mice. We propose that despite increased capacity for FAO in the diabetic heart, increased fatty acid uptake in hyperlipidemic states, such as that seen in uncontrolled diabetes, leads to a positive cellular lipid balance and cardiomyopathy in the diabetic.

How do alterations in myocardial lipid homeostasis lead to cardiomyopathy? Many potential mechanisms are possible, including direct toxic effects of neutral lipid droplets or fatty acid moieties on myofibrillar function (22), generation of toxic byproducts of mitochondrial or peroxisomal oxidation such as reactive oxygen species (16), increased oxygen consumption costs, or fatty acid-induced apoptosis (19, 20). In addition, alterations in cellular lipid metabolism could lead to activation of signaling pathways related to myocyte dysfunction, such as protein kinase C- or ceramide-mediated events. Although we cannot completely exclude any of these possible mechanisms, our data shed some light. Somewhat surprisingly, we did not find evidence of significant cell death or myocyte dropout in the MHC-PPAR/insulin-deficient model. Indeed, in the time frame studied, the cardiotoxicity was reversible. Secondly, the cardiomyopathy was worsened by inhibition of LCFA import into the mitochondria, indicating that metabolic events upstream of the mitochondria are involved. Given the dependence of the cardiomyopathic effects on LCFA and increased PPARα activity, we hypothesized that peroxisomal oxidative pathways could be involved in the generation of toxic intermediates. In support of this possibility, we found that the expression of the gene encoding ACO, a key enzyme in the peroxisomal FAO pathway and known PPARα target, was induced in MHC-PPAR and diabetic heart but not in PPAR$\alpha^{-/-}$ mice rendered diabetic. Levels of H_2O_2, a by-product of the reaction catalyzed by ACO, were increased in MHC-PPAR and diabetic PPAR$\alpha^{+/+}$ mice but not in diabetic PPAR$\alpha^{-/-}$ mice. In addition, the GSH/GSSG ratio was decreased in the hearts of HF-fed MHC-PPAR mice. These results raise the intriguing possibility that peroxisomal generation of H_2O_2 leads to myocyte hypertrophy and dysfunction. However, our data do not exclude a role for mitochondrial-generated reactive species, given that we have not evaluated the effects of blocking peroxisomal flux.

Perhaps the most intriguing and promising result of the current study was that the HF diet-induced cardiomyopathy of MHC-PPAR mice is reversible. Moreover, administration of an HF diet enriched in MCT improved the baseline LV dysfunction of MHC-PPAR mice. These results not only underscore the critical role of LCFA moieties in the cardiomyopathic phenotype, but suggest that pharmacologic or dietary lipid-lowering strategies may improve or prevent diabetic cardiomyopathy. Interestingly, in diabetic humans, high plasma TAG levels have been identified as a robust predictor of cardiovascular disease (23), and strategies to lower plasma lipid levels have been shown to improve cardiac function in diabetic rodents (24, 25). PPARα-activating ligands, such as clofibrate and gemfibrozil, are among the therapeutic agents known to reduce circulating TAG-rich lipoprotein levels. PPARα activators likely reduce plasma TAG levels by increasing the rate of hepatic fatty acid utilization and reducing very low density lipoprotein production. Although the use of PPARα activators seems counterintuitive in light of the current findings, the benefit of reduced delivery of fatty acids to the myocardium may outweigh the effects of activating the cardiac PPARα pathway in the diabetic patient. The use of the thiazolidinedione class of PPARγ activators as insulin sensitizers may also influence the development and severity of diabetic cardiomyopathy by reducing delivery of fatty acids to the myocardium. Our results suggest that the use of PPARα and -γ activators or related compounds as therapeutic agents will require rigorous evaluation of effects on cardiac function in the diabetic patient.

We thank Mary Wingate for assistance with manuscript preparation. All histological studies were performed in the Digestive Diseases Research Core Center at Washington University. B.N.F. is supported by National Research Service Award F32 HL67575 from the National Heart, Lung, and Blood Institute of the National Institutes of Health. This work was supported by National Institutes of Health Grants RO1 DK45416, P30 DK56341, P30 DK52574, PO1 HL57278, and PO1 HL13851.

1. Rubler, S., Dlugash, J., Yuceoglu, Y. Z., Kumral, T., Branwood, A. W. & Grishman, A. (1972) *Am. J. Cardiol.* **30,** 595–602.
2. Stone, P. H., Muller, J. E., Hartwell, T., York, B. J., Rutherford, J. D., Parker, C. B., Turi, Z. G., Strauss, H. W., Willerson, J. T. & Robertson, T. (1989) *J. Am. Coll. Cardiol.* **14,** 49–57.
3. Neely, J. R., Rovetto, M. J. & Oram, J. F. (1972) *Prog. Cardiovasc. Dis.* **15,** 289–329.
4. Lopaschuk, G. D. & Spafford, M. (1989) *Circ. Res.* **65,** 378–387.
5. Belke, D. D., Larsen, T. S., Gibbs, E. M. & Severson, D. L. (2000) *Am. J. Physiol.* **279,** E1104–E1113.
6. Finck, B., Lehman, J. J., Leone, T. C., Welch, M. J., Bennett, M. J., Kovacs, A., Han, X., Gross, R. W., Kozak, R., Lopaschuk, G. D. & Kelly, D. P. (2002) *J. Clin. Invest.* **109,** 121–130.
7. Desvergne, B. & Wahli, W. (1999) *Endocr. Rev.* **20,** 649–688.
8. Barger, P. M. & Kelly, D. P. (2000) *Trends Cardiovasc. Med.* **10,** 238–245.
9. Lee, S. S. T., Pineau, T., Drago, J., Lee, E. J., Owens, J. W., Kroetz, D. L., Fernandez-Salguero, P. M., Westphal, H. & Gonzalez, F. J. (1995) *Mol. Cell. Biol.* **15,** 3012–3022.
10. Xu, H., Guo, W. & Nerbonne, J. M. (1999) *J. Gen. Physiol.* **113,** 661–678.
11. Rogers, J. H., Tamirisa, P., Kovacs, A., Weinheimer, C., Courtois, M., Blumer, K. J., Kelly, D. P. & Muslin, A. J. (1999) *J. Clin. Invest.* **104,** 567–576.
12. Han, X. & Gross, R. W. (2001) *Anal. Biochem.* **295,** 88–100.
13. Han, X. (2002) *Anal. Biochem.* **302,** 199–212.
14. Kelly, D. P., Gordon, J. I., Alpers, R. & Strauss, A. W. (1989) *J. Biol. Chem.* **264,** 18921–18925.
15. Pick, E. & Keisari, Y. (1980) *J. Immunol. Methods* **38,** 161–170.
16. Liang, Q., Carlson, E. C., Donthi, R. V., Kralik, P. M., Shen, X. & Epstein, P. N. (2002) *Diabetes* **51,** 174–181.
17. Murthy, V. K. & Shipp, J. C. (1977) *Diabetes* **26,** 222–229.
18. Paulson, D. J. & Crass, M. F. (1982) *Am. J. Physiol.* **242,** 1084–1094.
19. Zhou, Y. T., Grayburn, P., Karim, A., Shimabukuro, M., Higa, M., Baetens, D., Orci, L. & Unger, R. H. (2000) *Proc. Natl. Acad. Sci. USA* **97,** 1784–1789.
20. Chiu, H.-C., Kovacs, A., Ford, D. A., Hsu, F.-F., Garcia, R., Herrero, P., Saffitz, J. E. & Schaffer, J. E. (2001) *J. Clin. Invest.* **107,** 813–822.
21. Nicholl, T. A., Lopaschuk, G. D. & McNeill, J. H. (1991) *Am. J. Physiol.* **261,** H1053–H1059.
22. Dyntar, D., Eppenberger-Eberhardt, M., Maedler, K., Pruschy, M., Eppenberger, H. M., Spinas, G. A. & Donath, M. Y. (2001) *Diabetes* **50,** 2105–2113.
23. West, K. M., Ahuja, M. M., Bennett, P. H., Czyzyk, A., DeAcosta, O. M., Fuller, J. H., Grab, B., Grabauskas, V., Jarrett, R. J. & Kosaka, K. (1983) *Diabetes Care* **6,** 361–369.
24. Heyliger, C. E., Rodrigues, B. & McNeill, J. H. (1986) *Diabetes* **35,** 1152–1157.
25. Rodrigues, B., Xiang, H. & McNeill, J. H. (1988) *Diabetes* **37,** 1358–1364.